

OccDepth: A Depth-Aware Method for 3D Semantic Scene Completion

Ruihang Miao*, Weizhou Liu*, Mingrui Chen, Zheng Gong, Weixin Xu, Chen Hu†, Shuchang Zhou
MEGVII Technology

Abstract

3D Semantic Scene Completion (SSC) can provide dense geometric and semantic scene representations, which can be applied in the field of autonomous driving and robotic systems. It is challenging to estimate the complete geometry and semantics of a scene solely from visual images, and accurate depth information is crucial for restoring 3D geometry. In this paper, we propose the first stereo SSC method named OccDepth, which fully exploits implicit depth information from stereo images (or RGBD images) to help the recovery of 3D geometric structures. The Stereo Soft Feature Assignment (Stereo-SFA) module is proposed to better fuse 3D depth-aware features by implicitly learning the correlation between stereo images. In particular, when the input are RGBD image, a virtual stereo images can be generated through original RGB image and depth map. Besides, the Occupancy Aware Depth (OAD) module is used to obtain geometry-aware 3D features by knowledge distillation using pre-trained depth models. In addition, a reformed TartanAir benchmark, named SemanticTartanAir, is provided in this paper for further testing our OccDepth method on SSC task. Compared with the state-of-the-art RGB-inferred SSC method, extensive experiments on SemanticKITTI show that our OccDepth method achieves superior performance with improving +4.82% mIoU, of which +2.49% mIoU comes from stereo images and +2.33% mIoU comes from our proposed depth-aware method. Our code and trained models are available at <https://github.com/megvii-research/OccDepth>.

1 Introduction

Humans can use their eyes to construct geometric and semantic information in 3D scenes, which can effectively help humans interact with 3D worlds. Dense representations of 3D scenes such as occupancy, dense point clouds, SDF [Park *et*

*Equal contribution.

†Corresponding authors.

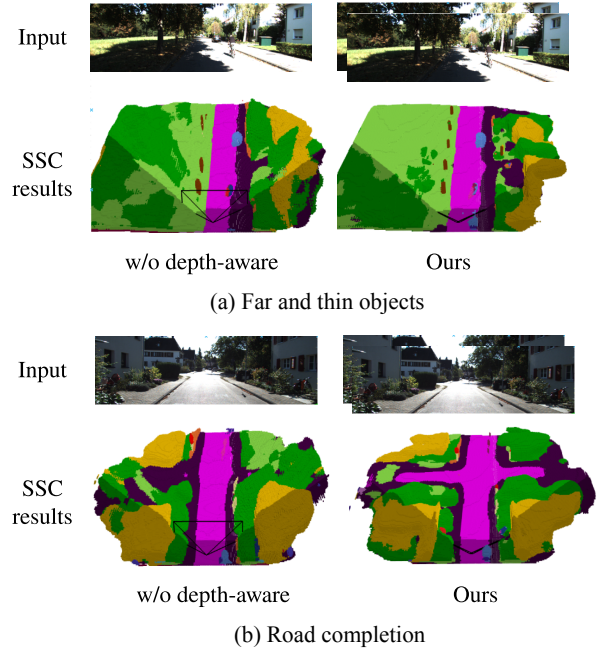


Figure 1: RGB based Semantic Scene Completion with/without depth-aware. (a) Our proposed OccDepth method can detect smaller and farther objects. (b) Our proposed OccDepth method complete road better.

al., 2019], etc. are useful for agents to perform various high-level tasks in a refined manner. Recently, we have witnessed great progress on these tasks, including path planning and environment interaction tasks. Numerous schemes have begun to explore the use of pure vision to restore dense 3D geometric structures and semantic information. However, restoring 3D structures from 2D images remains a challenging problem.

The 3D Semantic Scene Completion (SSC) task [Roldao *et al.*, 2022] attempts to reconstruct geometric and semantic structures based on observations and to complete occluded regions based on priors. The majority of the currently used 3D SSC technique depends on the input of 3D signals with depth information, such as voxels, point clouds, depth maps, and TSDF, which require expensive sensors to obtain. It is

desired to explore schemes that are based on cheaper and easy-to-deploy image sensors. Accurate depth information is crucial for the reconstruction and prediction of 3D geometric structures, while pure vision solutions frequently lack it. In the field of 3D detection, the accuracy of the pure vision solution is already competitive with the lidar solution. After the depth information is added to the 3D detection, it can be further improved, such as BEVDepth [Li *et al.*, 2022b]. Therefore, we aim to reduce the gap between vision-only and 3D input solutions by using depth information to enhance the performance of pure vision for SSC task.

In this paper, we explore how to exploit implicit depth information in images to help 3D SSC recover reliable geometry. Therefore, we introduce OccDepth, which is the first stereo 3D SSC method with vision-only input. In order to effectively use depth information, a Stereo Soft Feature Assignment (Stereo-SFA) module is proposed to better fuse 3D depth-aware features by implicitly learning the correlation between stereo images. An Occupancy Aware Depth (OAD) module uses knowledge distillation explicitly with pre-trained depth models to produce depth-aware 3D features. Additionally, we propose the SemanticTartanAir dataset based on TartanAir in order to validate the stereo-input scene more effectively. This is a virtual scene where real ground truth can be used to better evaluate the effectiveness of the method. Experiments show that our OccDepth method achieves superior performance on both SemanticKitti, NYUv2, and SemanticTartanAir benchmarks. Figure 1 shows the visualized results of OccDepth. With only images input, OccDepth can reconstruct thin objects, far objects, and objects with distinct geometric structures better. In summary, the main contributions are as follows:

- A Stereo Soft Feature Assignment (Stereo-SFA) module that better fuses 3D depth-aware features by implicitly learning correlation between stereo images.
- An Occupancy Aware Depth (OAD) module that uses knowledge distillation explicitly with pre-trained depth models to produce depth-aware 3D features.
- Our experiments show that our OccDepth method outperforms all vision-only baseline methods by a large margin and is close to the 3D input solutions.

2 Related works

3D Reconstruction From Images is a long-standing problem. Early methods use shape-from-shading [Drouot *et al.*, 2008] or structure-from-motion [Schonberger and Frahm, 2016; Cui *et al.*, 2017]. Recent neural radiance fields (NeRF) based methods [Mildenhall *et al.*, 2021] learn the density and color fields of 3D scenes. Built on the generalizable SceneRF [Cao and de Charette, 2022b] introduces a probabilistic ray sampling strategy and a spherical U-Net, to reconstruct large scenes using only single view as input. In addition to the above 3D reconstruction task, Scene Completion (SC) infers the complete geometry of a scene given images and/or 3D sparse inputs. SG-NN [Dai *et al.*, 2020] converts partial and noisy RGB-D scans into high-quality 3D scenes. Recently, [Engelmann *et al.*, 2021; Li and Cheng, 2021;

Liu and Liu, 2021; Sharma *et al.*, 2022] start to explore the 3D Semantic Instance Completion task, in which the object instances and their reconstructions are predicted from partial observations of the scene. In our work, we focus on the completion of geometry and semantics, named 3D SSC, that provides useful information for high-level tasks.

3D SSC is introduced in SSCNet [Song *et al.*, 2017], which shows that learning semantic segmentation and scene completion can mutually benefit. SSCNet takes a single RGB-D image as input and outputs a 3D voxel representation of occupancy and semantic labels. Following SSCNet, [Garbade *et al.*, 2019; Li *et al.*, 2020] leverage the depth and semantic information to achieve a better SSC result. Moreover, [Tang *et al.*, 2022] transfers voxels to point clouds to reduce the computation redundancy, and then fuses the voxel and the point stream using the proposed anisotropic voxel aggregation operator. In addition to the RGB-D based SSC methods, works [Cheng *et al.*, 2021; Wu *et al.*, 2020; Yang *et al.*, 2021; Yan *et al.*, 2021; Rist *et al.*, 2021] based on geometrical inputs (depth, point cloud or occupancy grids) are also proposed. Recently, [Dahnert *et al.*, 2021], an only RGB image based method, unifies the tasks of geometric reconstruction, 3D semantic segmentation, and 3D instance segmentation of indoor scenes from a single RGB image. MonoScene [Cao and de Charette, 2022a] infers dense 3D voxelized semantic indoor and outdoor scenes from a single RGB image. Similar to MonoScene, we use multiview RGB images to estimate dense geometry and semantics for indoor and outdoor scenes.

Knowledge Distillation is initially proposed in [Hinton *et al.*, 2015]. The main idea is to transfer the learned knowledge from a teacher network to a student one. Such a transference can be achieved by the soft targets of the output layer [Hinton *et al.*, 2015], the intermediate feature map [Romero *et al.*, 2014] and the activation status of each neuron [Huang and Wang, 2017]. Knowledge distillation has been widely investigated in a variety of computer vision tasks, such as semantic segmentation [Hou *et al.*, 2020; Liu *et al.*, 2019], 3D object detection [Chong *et al.*, 2022; Zheng *et al.*, 2022] and depth prediction [Pilzer *et al.*, 2019; Ye *et al.*, 2019]. Among the depth prediction methods, BEVDepth [Li *et al.*, 2022b] leverages explicit depth supervision through the sparse depth information from LiDAR to improve the accuracy of depth prediction. Different from BEVDepth, we utilize the explicit dense multiview stereo depth to teach the OAD module learn the depth prediction capability, which is more effective for stereo image inputs.

3 Methods

3.1 Overview

The overall processing pipeline of our OccDepth network is shown in Figure 2. Stereo images I_l, I_r are taken as inputs and are encoded into 2D features $\mathbf{F}_{2D,l}, \mathbf{F}_{2D,r} \in \mathbb{R}^{H \times W \times C}$. Then the 2D features are fused into 3D voxels, where the implicit depth information is embedded through a stereo soft feature assignment (Stereo-SFA) module. Next the explicit depth information is added into 3D features through an occupancy aware depth (OAD) module. Subsequently, during calculating the loss, the overall semantic scene completion

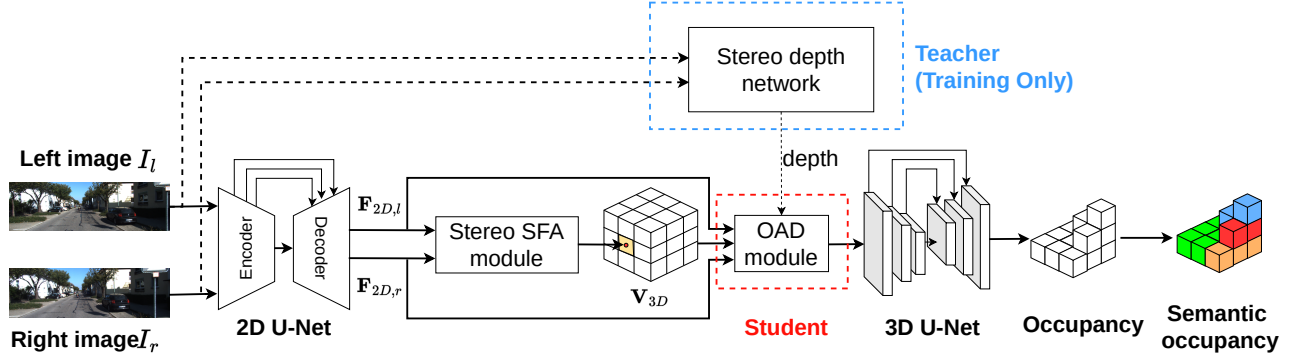


Figure 2: The process pipeline of the proposed OccDepth. The 3D SSC is inferred from stereo images with bridging a Stereo-SFA module to lift features to 3D space, an OAD module to enhance depth prediction, and a 3D U-Net to extract geometry and semantics. The stereo depth network is only used in training for giving a depth supervision.

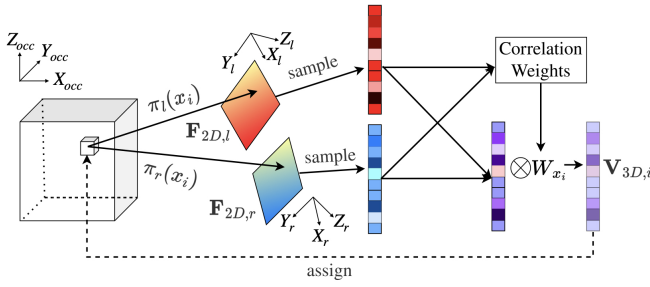


Figure 3: The illustration of stereo soft feature assignment module. The sampled 2D features are fused to 3D voxel feature.

loss are decoupled into geometric loss and semantic loss for better prediction. At last, a voxelized 3D scene \hat{y} with class labels $\mathcal{C} = \{c_0, c_1, \dots, c_N\}$ is predicted, where N is the total number of the semantic classes. As "empty" can also be regarded as a semantic class, c_0 represents empty voxels.

The rest of this section will describe the Stereo-SFA module (Sec. 3.2), OAD module (Sec. 4), losses (Sec. 3.4) and tricks for mitigating over-fitting (Sec. 3.5).

3.2 Stereo Soft Feature Assignment Module

In semantic occupancy predicting task, designing a good 2D-3D lifting function is a critical problem, especially when there is no direct depth information. While taking monocular image as input, the scale ambiguity is hard to handle when lifting 2D to 3D [Fahim et al., 2021]. Different from monocular image, the stereo image can provide implicit depth information that solves the scale ambiguity to a certain extent.

In order to calculate representation features of each voxel in the bounded 3D scene, the feature mapping between 2D image features and voxel features are needed. Unlike LSS [Phillon and Fidler, 2020] which implicitly unprojects 2D features to 3D space, we choose to project each voxel to the corresponding image pixel as done in MonoScene [Cao and de Charette, 2022a], which establishes a full feature mapping for all voxels. Moreover, the implicit depth information, which is derived through calculating the correlation between the left and right 2D features, is encoded as the weights of

3D features. Ablation in Sec. 4.3 shows that the above proposed feature mapping method is better than directly using stereo depth and is better than using a combination of left 2D features and right 2D features.

Figure 3 shows the process of Stereo-SFA module. Assuming that the stereo cameras has been calibrated and the input images have been undistorted, the intrinsic and extrinsic matrices of stereo cameras are known. Given $X \times Y \times Z$ voxels with centroid at coordinate $\mathbf{x} \in \mathbb{R}^{X \times Y \times Z \times 3}$, the 3D-2D projecting can be denoted as $\pi(\mathbf{x})$. Then, the 3D voxel feature $\mathbf{V}_{3D} \in \mathbb{R}^{X \times Y \times Z \times C}$ can be sampled from corresponding 2D feature map \mathbf{F}_{2D} and written as

$$\mathbf{V}_{3D} = \phi_{\pi(\mathbf{x})}(\mathbf{F}_{2D}), \quad (1)$$

where $\phi_{\mathbf{x}}(M)$ is the sampling function that sample feature mapping M at coordinates \mathbf{x} . The 3D features will be set as $\mathbf{0}$ when the projected 2D points are out of the image.

Denoting $\mathbf{V}_{3D,l}$ and $\mathbf{V}_{3D,r}$ as the 3D features acquired from the left 2D feature map and the right 2d feature map respectively, the weighted 3D feature $\mathbf{V}_{3D,w}$ is written as

$$\mathbf{V}_{3D,w} = \begin{cases} \mathbf{V}_{3D,l}, & \text{if } \mathbf{V}_{3D,r} = \mathbf{0} \\ \mathbf{V}_{3D,r}, & \text{if } \mathbf{V}_{3D,l} = \mathbf{0} \\ w \times \frac{\mathbf{V}_{3D,l} + \mathbf{V}_{3D,r}}{2}, & \text{others} \end{cases}, \quad (2)$$

where w denotes the weights calculated from the correlation between $\mathbf{V}_{3D,l}$ and $\mathbf{V}_{3D,r}$. In this paper, the cosine similarity is used to measure the correlation of features. In order to enlarge the receptive field, the multi-scale 2D feature maps are considered. The output 3D feature map is written as

$$\mathbf{V}_{3D} = \sum_{s \in \mathcal{S}} \mathbf{V}_{3D,w}^s, \quad (3)$$

where $\mathcal{S} = \{1, 2, 4, 8\}$ is a set of downsampling scales.

3.3 Occupancy-Aware Depth Module

Module Structure

In order to introduce spatial occupancy prior information when converting 2D image feature to 3D voxel feature, the

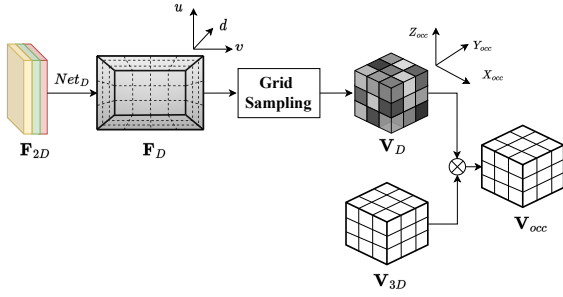


Figure 4: The illustration of the occupancy aware depth module. For simplicity, only the processing flow of single-shot V_D is shown. The OAD module is used to introduce spatial occupancy prior by the predicted depth information.

OAD module is proposed. Inspired by the excellent 3D object detection works [Li *et al.*, 2022a; Reading *et al.*, 2021], the OAD module uses the predicted depth information to estimate the prior probability of the existence of objects in the voxel feature space. This probability information is then used to improve the spatial information of voxel features.

Figure 4 shows the process of our occupancy aware depth module. Through the above Stereo-SFA module, the corresponding stereo feature maps in the voxel space $V_{3D} \in \mathbb{R}^{X \times Y \times Z \times C}$ are obtained. The single scale image feature $F_{2D} \in \mathbb{R}^{H \times W \times C}$ with downsampling scale S is fed to the OAD module, where S is set to be 8. Firstly, a depth distribution network Net_D is used to predict the depth feature $F_D \in \mathbb{R}^{C \times H \times W \times D}$ of the multi-view input images. Secondly, a softmax operator is used to transform the F_D into frustum depth distribution $G_D \in \mathbb{R}^{H \times W \times D}$, where the categories are the D discretized depth bins. Thirdly, the frustum depth distribution G_D is transformed to a voxel-space depth distribution representation $V_D \in \mathbb{R}^{X \times Y \times Z}$ with the differentiable grid sampling process, using the camera calibration matrix $P \in \mathbb{R}^{3 \times 4}$. There are several depth discretization methods: uniform discretization (UD), linear-increasing discretization (LID) [Tang *et al.*, 2021] and spacing-increasing discretization (SID) [Fu *et al.*, 2018]. We utilize LID in depth discretization process as it provides a more refined expression for the near space. LID is defined as:

$$d_c = d_{min} + \frac{d_{max} - d_{min}}{D \cdot (D + 1)} \cdot d_i \cdot (d_i + 1), \quad (4)$$

where d_c and d_i are continuous depth value and discretized depth bin index, $[d_{min}, d_{max}]$ is the full depth range, and D is the number of target discretized bins. Finally, the occupancy aware voxel feature V_{occ} can be obtained:

$$V_{occ} = \left(\sum_i^2 V_D^i \cdot M \right) \cdot V_{3D}, \quad (5)$$

where M is the mask for averaging the voxel pixel in the overlap region between stereo inputs, the value in overlap region is 0.5 and others is 1.0, and V_D can be represented as occupancy probability prior in voxel space.

Stereo Depth Distillation

In the above mentioned module, the depth distribution network Net_D is trained based on implicit supervision, where the gradient comes from the back propagation process of occupancy related loss. Because the 2D to 3D transformation process mentioned above is highly dependent on the performance of the predicted depth distribution. Inspired by BevDepth [Li *et al.*, 2022b], stereo depth distillation is adopted in the training process to help the depth distribution network Net_D have better depth estimation performance. Stereo depth distillation introduces explicit supervision on the depth feature F_D . Different from the BevDepth that uses the sparse lidar point cloud to generate ground truth depth, our ground truth depth D_{GT} with more dense information is generated by a stereo depth network LEAStereo. To align the ground truth depth with the predicted depth feature F_D , a *min pooling* and a *one hot* operator are adopted on D_{GT} to generate F_{GT_D} . Finally, binary cross entropy is adopted to calculate the depth loss:

$$L_{depth} = \psi(F_D, F_{GT_D}), \quad (6)$$

where ψ is the cross-entropy loss function.

3.4 Losses

As the semantic scene completion task can be decomposed into the occupancy prediction task and the semantic prediction task. Inspired by [Chen *et al.*, 2020], we solve the geometric prediction task and the semantic prediction task step by step. Firstly, the V_{3D} generated from 3D U-Net structure can be processed to F_{3D}^{2class} with a single 3D convolutional layer, where the F_{3D}^{2class} is used to predict whether each element in the voxel is occupied. The F_{3D}^{2class} is used to generate occupancy loss:

$$L_{occ} = \psi(F_{3D}^{2class}, GT_{3D}^{geo}), \quad (7)$$

where GT_{3D}^{geo} is the geometric ground truth with 2 classes, the first class represents the empty voxel and the second class represents the voxel that is occupied, and ψ is the binary cross-entropy loss function. Secondly, the F_{3D} and F_{3D}^{2class} are concatenated as F_{3D}^{occ} , and F_{3D}^{Nclass} is generated with a single 3d convolutional layer. The F_{3D}^{Nclass} is used to generate semantic loss:

$$L_{sem} = \psi(F_{3D}^{Nclass}, GT_{3D}^{sem}), \quad (8)$$

where GT_{3D}^{sem} is the semantic ground truth with N classes corresponded to the dataset definition, and ψ is the cross-entropy loss function.

Refer to the definition of losses in Monoscene [Cao and de Charette, 2022a], L_{mono} loss is also used in the OccDepth training process. The L_{mono} is defined as:

$$L_{mono} = L_{rel} + L_{scal}^{sem} + L_{scal}^{geo} + L_{fp}. \quad (9)$$

where the L_{rel} is helpful for capturing better semantic information, the L_{scal}^{sem} and L_{scal}^{geo} are helpful for semantic and geometric accuracy improvement and the L_{fp} is used to improve the completion ability. So the OccDepth is trained by optimizing the following loss:

$$L_{total} = L_{occ} + L_{sem} + L_{depth} + L_{mono}. \quad (10)$$

Method	Input	SC IoU	SSC mIoU
2.5D/3D			
LMSCNet st	OCC	33.00	5.80
AICNet st	RGB, DEPTH	32.8	6.80
JS3CNet st	PTS	39.30	9.10
2D			
MonoScene	RGB	34.16	11.08
MonoScene st	Stereo RGB	40.84	13.57
OccDepth (ours)	Stereo RGB	45.10	15.90

(a) SemanticKITTI (hidden test set)

Method	Input	SC IoU	SSC mIoU
2.5D/3D			
LMSCNet st	OCC	37.63	12.38
AICNet st	RGB, DEPTH	31.86	10.03
JS3CNet st	PTS	26.81	9.55
3DSketch st	RGB, TSDF	62.46	25.79
2D			
MonoScene	RGB	34.87	24.12
MonoScene st	Stereo RGB	49.63	32.79
OccDepth (ours)	Stereo RGB	52.49	34.96

(b) SemanticTartanAir (test set)

Table 1: Performance on SemanticKITTI and SemanticTartanAir. The scene completion (SC IoU) and semantic scene completion (SSC mIoU) are reported for modified baselines (marked with superscript "st") and our OccDepth.

3.5 Tricks for Mitigating Over-fitting

Due to the large amount of model parameters including 3D convolutions and the small amount of training data, the training process is prone to over-fitting problems. Several tricks are proposed to mitigate the over-fitting problem.

- **2D Pre-training:** The 2D backbone in the OccDepth can be pre-trained on a large instance segmentation datasets, the pre-training process can enhance semantic information in 2d features (\mathbf{F}_{2D}).
- **Data Augmentation:** Stronger data augmentation can mitigate the problem of having less training data. We find that Gaussian blur, grayscale and hue adjustment are helpful augmentation methods.
- **Loss Weight Adjustment:** Due to the imbalance of loss scales of different tasks, some over-fitting losses can greatly reduce the optimization effect of other losses. The over-fitting loss L_{sem}^{scal} will be weighted by a gradually reduced weight γ in the training process. The γ is calculated as follows: $\gamma = \max(0.2, 1 - \frac{x}{N})$, where x is the current training step and N is the total training steps.

4 Experiments

OccDepth method is evaluated on SemanticKitti [Behley et al., 2019], NYUv2 [Silberman et al., 2012] and SemanticTar-

Method	SemanticKITTI		SemanticTartanAir		NYUv2	
	IoU	mIoU	IoU	mIoU	IoU	mIoU
2.5D/3D						
LMSCNet	56.7*	17.6*	92.2	36.5	44.1*	20.4*
JS3CNet	56.6*	23.8*	91.6	25.5	/	/
S3CNet	45.6*	29.5*	/	/	/	/
Local-DIFs	57.7*	22.7*	/	/	/	/
AICNet	/	/	99.0	40.0	43.9*	23.8*
3DSketch	/	/	91.6	31.5	49.5*	29.2*
2D						
MonoScene	34.2*	11.1*	34.9	24.1	42.1	26.5
OccDepth(ours)	45.1	15.9	52.5	35.0	50.3	30.9

Table 2: Baselines of 2.5D/3D-input methods. OccDepth outperforms some indoor baselines and is even comparable to some outdoor baselines. "*" means results are cited from MonoScene. "/" means missing results.

tanAir. The baseline methods are MonoScene [Cao and de Charette, 2022a] and the stereo adaptation version of recent 2.5D/3D-input based SSC methods. we train our model for 30 epochs with an AdamW [Loshchilov and Hutter, 2017] optimizer for all cases. The training hyper-parameters are: batchsize is 1, learning rate is 10^{-4} , weight decay is 10^{-4} . The learning rate is divided by 10 at epoch 20.

In the rest of this section, dataset and metrics are described in Sec. 4.1. Then the comparison results between our method and SOTA methods are showed in Sec. 4.2. Finally, the ablation study about proposed modules are presented in Sec. 4.3.

4.1 Datasets and Metric

Datasets. SemanticKITTI [Behley et al., 2019] dataset provided $256 \times 256 \times 32$ voxel grids labeled with 21 classes. The voxels are generated through post-processing the Lidar scans and the size of each voxel is $0.2m$. We use cam2 and cam3 as a stereo RGB camera. The official 3834/815 train/val splits are used in all evaluations. The evaluating results of quantitative analysis are acquired from the hidden test set and the evaluating results of ablation studies are acquired from the validation set.

NYUv2 [Silberman et al., 2012] dataset provided $240 \times 144 \times 240$ voxels grids labeled with 13 classes. 795/654 train/test splits are used in all evaluations as [Cao and de Charette, 2022a; Li et al., 2019]. The evaluation is taken on the downsampled test set with $60 \times 36 \times 60$ voxels. Because there is no stereo image on NYUv2, the Stereo-SFA module is removed in the experiments on NYUv2.

SemanticTartanAir dataset based on TartanAir [Wang et al., 2020] is collected in a simulation environments that provides multimodal sensor data, including stereo RGB images, depth maps, segmentations, LiDAR point clouds, with precise ground truth labels. Although TartanAir dataset covers a wide range of scenes, we only focus on the indoor scene. Thus, we generate $120 \times 48 \times 120$ voxel grids with 14 classes of semantic labels for each RGB image in office scene with the help of the depth maps. The size of each voxel is $0.1m$. In SemanticTartanAir benchmark, 1976/192 train/test splits are used.

Evaluation Metric. Following previous works, the intersection over union (IoU) of occupied voxels and the mean

IoU (mIoU) of semantic classes are reported for evaluating SC task and SSC task, respectively. In all datasets, the IoU and mIoU is calculated through on all voxels of the scene.

4.2 Comparison to State-of-the-arts

We compare OccDepth with state-of-the-art SSC methods. These methods can be classified as RGB-inferred methods and 2.5D/3D-input methods.

Comparison with stereo-based methods. The performance of OccDepth on SemanticKITTI (hidden test set) and SemanticTartanAir (test set) is reported in Table 1. All of the 2.5D/3D-input baseline methods are modified to stereo RGB-inferred version which are marked with superscript "st". Stereo images are used to generate occupancy, TSDF, point clouds and depth maps for 2.5D/3D-input baselines methods. For the monocular-based MonoScene [Cao and de Charette, 2022a], we fused 3D voxel features by average from stereo inputs, which named MonoScenest. The best results are shown in bold. As there is no stereo images in NYUv2 dataset, we only compare OccDepth with the original baselines in Table 2. The experiment results demonstrate that our OccDepth outperforms other methods. Compared with MonoScene, which is a 2D baseline method, OccDepth improves about +4.82 mIoU/+10.94 IoU on SemanticKITTI (Table 1a) and +10.84 mIoU/+17.62 IoU on SemanticTartanAir (Table 1b). On SemanticKITTI, our OccDepth achieves much better results than MonoScenest. Furthermore, compared with MonoScenest, our OccDepth also achieves considerable improvements ([+2.33 mIoU, +4.26 IoU]). This implies that OccDepth can give more elaborate geometric structure than MonoScenest. On SemanticTartanAir, OccDepth achieves the best SSC mIoU with improvements (+2.17 mIoU) than MonoScenest. However, due to that 2.5D/3D methods have natural advantages on geometry, the SC IoU of OccDepth does not achieve the best.

Comparison with 2.5D/3D methods. We also compare OccDepth with the original 2.5D/3D input baselines. The results are listed in Table 2. In SemanticKITTI (hidden test set), though OccDepth only uses stereo images that has a much less horizontal field of view (FOV) than lidar (82° vs. 180°), OccDepth achieves comparable results with 2.5D/3D-input methods. This result demonstrates that OccDepth has a relatively better completion ability. In NYUv2 (test set), because there are no stereo images, our OccDepth generates virtual stereo images through RGB image and depth map. our OccDepth achieves the best mIoU and IoU ([+0.8 IoU, +1.7 mIoU]) than 2.5D/3D methods. In SemanticTartanAir (test set), we use GT depth as the input for these 2.5D/3D methods here, so the accuracy is very high. On the other hand, our OccDepth has a close mIoU result compared with 2.5D/3D-input methods while we do not use the GT depth. And compared with RGB-inferred method, our OccDepth has a much higher IoU and mIoU ([+17.6 IoU, +10.9 mIoU]).

Qualitative Results

We compare our SSC outputs with the above mentioned methods in Figure 5. To show the advantages of our method in visualization, the input image (leftmost column) and its corresponding ground truth (rightmost) are also listed.

Method	IoU ↑	mIoU ↑
Ours	45.25	16.20
Ours w/o TMO	45.05	15.80
Ours w/o Depth Distillation	45.03	15.29
Ours w/o OAD	44.97	14.63
Ours w/o Stereo-SFA	42.99	14.11
MonoScene [Cao and de Charette, 2022a]	37.12	11.50

Table 3: Architecture ablation. Results are reported on SemanticKITTI *val*.

On indoor scenes (SemanticTartanAir, Figure 5a), although all methods correctly capture global scene layouts, OccDepth has better restoration effect of object edges, such as sofa (row 1) and ceiling lights (row 2) and carpet (row 3).

On outdoor scenes (SemanticKITTI, Figure 5b), compared to baseline methods, the spatial and semantic prediction results of OccDepth are obviously better. For example, accurate identification of road signs (row 1), trunk (row 2), vehicle (row 2) and road (row 3) can be achieved by OccDepth.

4.3 Ablation Study

Architectural Components

Table 3 shows that all architectural components contribute to the best results. The MonoScene experiment shows the accuracy of single-view baseline. For "Ours w/o Stereo-SFA", the multi-view fusion process is conducted by a naive average operator. When we use Stereo-SFA (Sec. 3) for multi-view fusion, the accuracy has been significantly improved ([+1.98 IoU, +0.52 mIoU]). The OAD (Sec. 4) module also contributes to accuracy improvement ([+0.06 IoU, +0.65 mIoU]). And the depth distillation (Sec. 4) with stereo depth data can further improve the accuracy ([+0.02 IoU, +0.51 mIoU]). Finally, the best accuracy ([+0.02 IoU, +0.51 mIoU]) can be obtained with tricks of the mitigating over-fitting (Sec. 3.5).

Though Stereo-SFA module brings significant improvements on both IoU and mIoU, it also increases the amount of computation by 42%. In contrast, the OAD module only brings significant improvement on mIoU with almost no increase in computation.

Effectiveness of Stereo-SFA module

We ablate our Stereo-SFA module on SemanticKITTI (*validation set*) to show the advantages of Stereo-SFA module. 2D U-Net based on pre-trained EfficientNet-B3 [Tan and Le, 2019] is used to generate 2D features with feature channels 24. Table 4a shows SC IoU and SSC mIoU results of different stereo fusion methods. The "Mean" fusion method means that the average value of left 2D feature and right 2D feature is assigned to corresponding voxel. We also implemented a better fusion method named "Concat" in Table 4a. The "Concat" fusion method fuses feature through concatenating the left 2D feature and right 2D feature followed by a 1:2 downsampling. The results show Stereo-SFA is better than "Mean" fusion method with improvements of +2.96 IoU/+0.76 mIoU and is better than "Concat" fusion method with improvement of +1.30 IoU/+0.05 mIoU. Note that Stereo-SFA fusion method significantly improves the SC IoU. And the improvement on

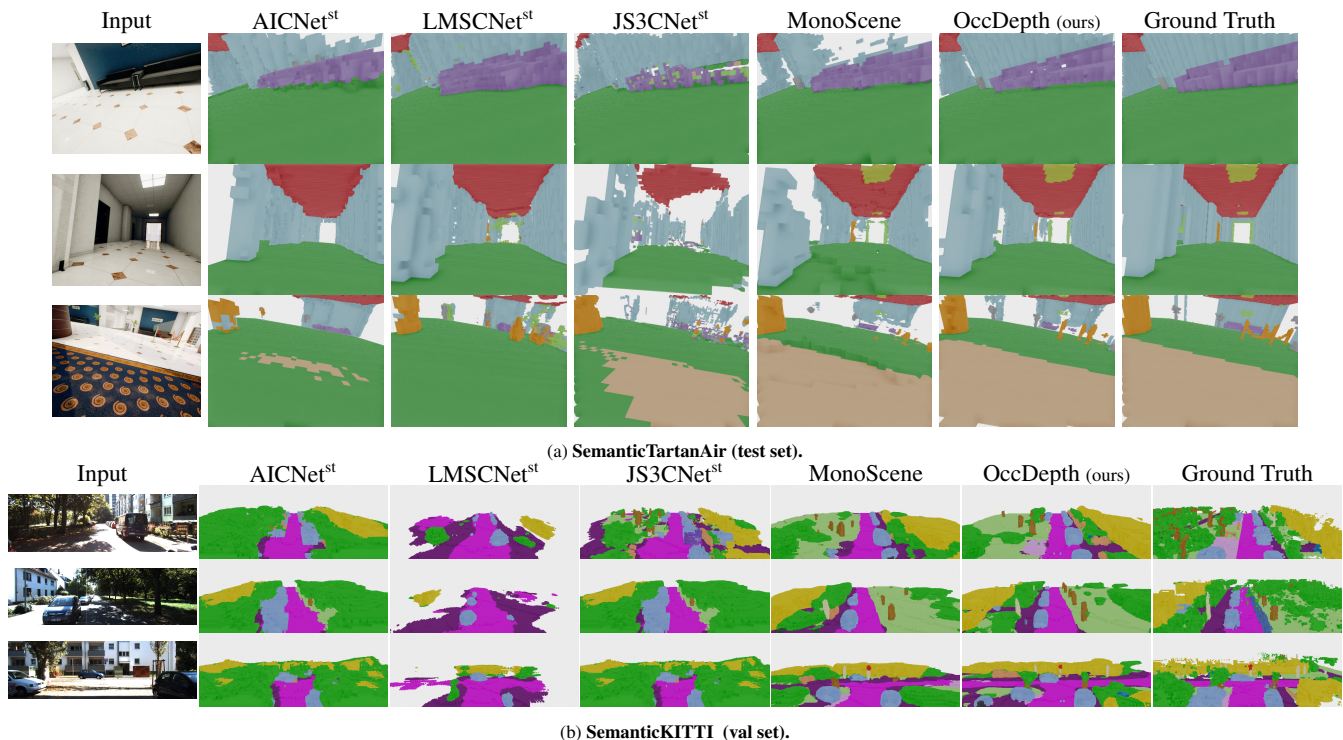


Figure 5: Qualitative study on (a) SemanticTartanAir and (b) SemanticKITTI. The input is shown on the leftmost and the ground truth is shown on the rightmost. OccDepth captures better scene layout on both datasets.

Fusion methods	IoU \uparrow	mIoU \uparrow
Mean	39.64	12.39
Concat	41.30	13.10
Stereo-SFA	42.60	13.15

(a) Stereo-SFA module.

Depth Discretization Method	IoU \uparrow	mIoU \uparrow
UD	35.36	10.00
SID [Fu <i>et al.</i> , 2018]	35.30	10.15
LID [Tang <i>et al.</i> , 2021]	35.61	10.18

(b) Depth discretization methods.

Depth Distillation Data Source	IoU \uparrow	mIoU \uparrow
w/o Depth	45.03	15.30
Lidar Depth	43.86	15.19
Stereo Depth	45.05	15.80

(c) Depth distillation data source.

Table 4: Ablation study of proposed modules. (a) Ablation study of Stereo-SFA module. (b) Ablation study of Depth distillation data source in OAD module. (c) Ablation study of Depth distillation data source in OAD module. w/o Depth means no depth distillation is used, Lidar depth refers to the depth image generated by lidar point cloud and Stereo Depth refers to the depth image generated by LEAStereo model. Results are reported on SemanticKITTI *val*.

SC IoU proves that the geometric information is more effectively introduced into the system by our Stereo-SFA module.

Effectiveness of OAD module

We provide ablation studies of OAD module to validate our design choices. The results are shown in Tables 4b and 4c. Experiment in Table 4b shows the experimental results of several different depth discretization methods. The comparison experiments are conducted with single-view image input, and the small model (EfficientNet-B3) with feature channels 24 are used to improve the efficiency of comparative experiments. Note that the LID depth discretization method achieves the highest accuracy. The SID depth discretization method also achieves comparable mIoU with LID depth discretization method since SID also spends more depth bin resources on nearby objects.

Experiment in Table 4c shows the experimental results of two different depth sources for depth distillation process. The lidar depth images are generated by a lidar point cloud projec-

tion process, so these depth images are sparse in image space. The stereo depth images are generated by the LEAStereo model, so the generated depth images are spatially dense due to the compensation Ability of Neural Networks. Our depth distillation method with lidar depth data achieves 15.19% mIoU, and achieves 15.80% mIoU with lidar depth data. A reasonable explanation for the results maybe the sparse property in image space leads to low accuracy.

5 Conclusion

In this paper, a depth-aware method for 3D SSC, which is named OccDepth, is presented. We trained OccDepth on public datasets including SemanticKITTI (outdoor scene) and NYUv2 (indoor scene) dataset. Experiment results demonstrate that OccDepth is comparable to some 2.5D/3D-input methods on both indoor scene and outdoor scene. Especially, OccDepth outperforms current RGB-inferred baselines on all classes. Moreover, the experiment results on newly proposed

indoor benchmark based on SemanticTartanAir verify the improvements of stereo input in indoor scene. As far as we know, OccDepth is the first stereo RGB-inferred method that is comparable to 2.5D/3D-input SSC methods.

References

- [Behley *et al.*, 2019] Jens Behley, Martin Garbade, Andres Milioto, Jan Quenzel, Sven Behnke, Cyrill Stachniss, and Jurgen Gall. Semantickitti: A dataset for semantic scene understanding of lidar sequences. In *Proceedings of the IEEE/CVF International Conference on Computer Vision*, pages 9297–9307, 2019.
- [Cao and de Charette, 2022a] Anh-Quan Cao and Raoul de Charette. Monoscene: Monocular 3d semantic scene completion. In *Proceedings of the IEEE/CVF Conference on Computer Vision and Pattern Recognition (CVPR)*, pages 3991–4001, June 2022.
- [Cao and de Charette, 2022b] Anh-Quan Cao and Raoul de Charette. Scenerf: Self-supervised monocular 3d scene reconstruction with radiance fields. *arXiv preprint arXiv:2212.02501*, 2022.
- [Chen *et al.*, 2020] Xiaokang Chen, Yajie Xing, and Gang Zeng. Real-time semantic scene completion via feature aggregation and conditioned prediction. In *2020 IEEE International Conference on Image Processing (ICIP)*, pages 2830–2834. IEEE, 2020.
- [Cheng *et al.*, 2021] Ran Cheng, Christopher Agia, Yuan Ren, Xinhai Li, and Liu Bingbing. S3cnet: A sparse semantic scene completion network for lidar point clouds. In *Conference on Robot Learning*, pages 2148–2161. PMLR, 2021.
- [Chong *et al.*, 2022] Zhiyu Chong, Xinzhu Ma, Hong Zhang, Yuxin Yue, Haojie Li, Zhihui Wang, and Wanli Ouyang. Monodistill: Learning spatial features for monocular 3d object detection. *arXiv preprint arXiv:2201.10830*, 2022.
- [Cui *et al.*, 2017] Hainan Cui, Xiang Gao, Shuhan Shen, and Zhanyi Hu. Hsfm: Hybrid structure-from-motion. In *Proceedings of the IEEE conference on computer vision and pattern recognition*, pages 1212–1221, 2017.
- [Dahnert *et al.*, 2021] Manuel Dahnert, Ji Hou, Matthias Nießner, and Angela Dai. Panoptic 3d scene reconstruction from a single rgb image. *Advances in Neural Information Processing Systems*, 34:8282–8293, 2021.
- [Dai *et al.*, 2020] Angela Dai, Christian Diller, and Matthias Nießner. Sg-nn: Sparse generative neural networks for self-supervised scene completion of rgb-d scans. In *Proceedings of the IEEE/CVF Conference on Computer Vision and Pattern Recognition*, pages 849–858, 2020.
- [Durou *et al.*, 2008] Jean-Denis Durou, Maurizio Falcone, and Manuela Sagona. Numerical methods for shape-from-shading: A new survey with benchmarks. *Computer Vision and Image Understanding*, 109(1):22–43, 2008.
- [Engelmann *et al.*, 2021] Francis Engelmann, Konstantinos Rematas, Bastian Leibe, and Vittorio Ferrari. From points to multi-object 3d reconstruction. In *Proceedings of the IEEE/CVF Conference on Computer Vision and Pattern Recognition*, pages 4588–4597, 2021.
- [Fahim *et al.*, 2021] George Fahim, Khalid Amin, and Sameh Zarif. Single-view 3d reconstruction: A survey of deep learning methods. *Computers & Graphics*, 94:164–190, 2021.
- [Fu *et al.*, 2018] Huan Fu, Mingming Gong, Chaohui Wang, Kayhan Batmanghelich, and Dacheng Tao. Deep ordinal regression network for monocular depth estimation. In *Proceedings of the IEEE conference on computer vision and pattern recognition*, pages 2002–2011, 2018.
- [Garbade *et al.*, 2019] Martin Garbade, Yueh-Tung Chen, Johann Sawatzky, and Jurgen Gall. Two stream 3d semantic scene completion. In *Proceedings of the IEEE/CVF Conference on Computer Vision and Pattern Recognition Workshops*, pages 0–0, 2019.
- [Hinton *et al.*, 2015] Geoffrey Hinton, Oriol Vinyals, Jeff Dean, et al. Distilling the knowledge in a neural network. *arXiv preprint arXiv:1503.02531*, 2(7), 2015.
- [Hou *et al.*, 2020] Yuenan Hou, Zheng Ma, Chunxiao Liu, Tak-Wai Hui, and Chen Change Loy. Inter-region affinity distillation for road marking segmentation. In *Proceedings of the IEEE/CVF Conference on Computer Vision and Pattern Recognition*, pages 12486–12495, 2020.
- [Huang and Wang, 2017] Zehao Huang and Naiyan Wang. Like what you like: Knowledge distill via neuron selectivity transfer. *arXiv preprint arXiv:1707.01219*, 2017.
- [Li and Cheng, 2021] Shichao Li and Kwang-Ting Cheng. Joint stereo 3d object detection and implicit surface reconstruction. *arXiv preprint arXiv:2111.12924*, 2021.
- [Li *et al.*, 2019] Jie Li, Yu Liu, Dong Gong, Qinfeng Shi, Xia Yuan, Chunxia Zhao, and Ian Reid. Rgbd based dimensional decomposition residual network for 3d semantic scene completion. In *Proceedings of the IEEE/CVF Conference on Computer Vision and Pattern Recognition*, pages 7693–7702, 2019.
- [Li *et al.*, 2020] Siqi Li, Changqing Zou, Yipeng Li, Xibin Zhao, and Yue Gao. Attention-based multi-modal fusion network for semantic scene completion. In *Proceedings of the AAAI Conference on Artificial Intelligence*, volume 34, pages 11402–11409, 2020.
- [Li *et al.*, 2022a] Yanwei Li, Yilun Chen, Xiaojuan Qi, Zeming Li, Jian Sun, and Jiaya Jia. Unifying voxel-based representation with transformer for 3d object detection. *arXiv preprint arXiv:2206.00630*, 2022.
- [Li *et al.*, 2022b] Yinhao Li, Zheng Ge, Guanyi Yu, Jinrong Yang, Zengran Wang, Yukang Shi, Jianjian Sun, and Zeming Li. Bevdepth: Acquisition of reliable depth for multi-view 3d object detection. *arXiv preprint arXiv:2206.10092*, 2022.
- [Liu and Liu, 2021] Feng Liu and Xiaoming Liu. Voxel-based 3d detection and reconstruction of multiple objects from a single image. *Advances in Neural Information Processing Systems*, 34:2413–2426, 2021.

- [Liu *et al.*, 2019] Yifan Liu, Ke Chen, Chris Liu, Zengchang Qin, Zhenbo Luo, and Jingdong Wang. Structured knowledge distillation for semantic segmentation. In *Proceedings of the IEEE/CVF Conference on Computer Vision and Pattern Recognition*, pages 2604–2613, 2019.
- [Loshchilov and Hutter, 2017] Ilya Loshchilov and Frank Hutter. Decoupled weight decay regularization. *arXiv preprint arXiv:1711.05101*, 2017.
- [Mildenhall *et al.*, 2021] Ben Mildenhall, Pratul P Srinivasan, Matthew Tancik, Jonathan T Barron, Ravi Ramamoorthi, and Ren Ng. Nerf: Representing scenes as neural radiance fields for view synthesis. *Communications of the ACM*, 65(1):99–106, 2021.
- [Park *et al.*, 2019] Jeong Joon Park, Peter Florence, Julian Straub, Richard Newcombe, and Steven Lovegrove. DeepSDF: Learning continuous signed distance functions for shape representation. In *Proceedings of the IEEE/CVF conference on computer vision and pattern recognition*, pages 165–174, 2019.
- [Phillion and Fidler, 2020] Jonah Phillion and Sanja Fidler. Lift, splat, shoot: Encoding images from arbitrary camera rigs by implicitly unprojecting to 3d. In *Proceedings of the European Conference on Computer Vision*, 2020.
- [Pilzer *et al.*, 2019] Andrea Pilzer, Stephane Lathuiliere, Nicu Sebe, and Elisa Ricci. Refine and distill: Exploiting cycle-inconsistency and knowledge distillation for unsupervised monocular depth estimation. In *Proceedings of the IEEE/CVF Conference on Computer Vision and Pattern Recognition*, pages 9768–9777, 2019.
- [Reading *et al.*, 2021] Cody Reading, Ali Harakeh, Julia Chae, and Steven L Waslander. Categorical depth distribution network for monocular 3d object detection. In *Proceedings of the IEEE/CVF Conference on Computer Vision and Pattern Recognition*, pages 8555–8564, 2021.
- [Rist *et al.*, 2021] Christoph Rist, David Emmerichs, MarkusENZweiler, and Dariu Gavrilă. Semantic scene completion using local deep implicit functions on lidar data. *IEEE Transactions on Pattern Analysis and Machine Intelligence*, 2021.
- [Roldao *et al.*, 2022] Luis Roldao, Raoul De Charette, and Anne Verroust-Blondet. 3d semantic scene completion: a survey. *International Journal of Computer Vision*, pages 1–28, 2022.
- [Romero *et al.*, 2014] Adriana Romero, Nicolas Ballas, Samira Ebrahimi Kahou, Antoine Chassang, Carlo Gatta, and Yoshua Bengio. Fitnets: Hints for thin deep nets. *arXiv preprint arXiv:1412.6550*, 2014.
- [Schonberger and Frahm, 2016] Johannes L Schonberger and Jan-Michael Frahm. Structure-from-motion revisited. In *Proceedings of the IEEE conference on computer vision and pattern recognition*, pages 4104–4113, 2016.
- [Sharma *et al.*, 2022] Prafull Sharma, Ayush Tewari, Yilun Du, Sergey Zakharov, Rares Ambrus, Adrien Gaidon, William T Freeman, Fredo Durand, Joshua B Tenenbaum, and Vincent Sitzmann. Seeing 3d objects in a single image via self-supervised static-dynamic disentanglement. *arXiv preprint arXiv:2207.11232*, 2022.
- [Silberman *et al.*, 2012] Nathan Silberman, Derek Hoiem, Pushmeet Kohli, and Rob Fergus. Indoor segmentation and support inference from rgbd images. In *European conference on computer vision*, pages 746–760. Springer, 2012.
- [Song *et al.*, 2017] Shuran Song, Fisher Yu, Andy Zeng, Angel X Chang, Manolis Savva, and Thomas Funkhouser. Semantic scene completion from a single depth image. In *Proceedings of the IEEE conference on computer vision and pattern recognition*, pages 1746–1754, 2017.
- [Tan and Le, 2019] Mingxing Tan and Quoc Le. EfficientNet: Rethinking model scaling for convolutional neural networks. In Kamalika Chaudhuri and Ruslan Salakhutdinov, editors, *Proceedings of the 36th International Conference on Machine Learning*, volume 97 of *Proceedings of Machine Learning Research*, pages 6105–6114. PMLR, 09–15 Jun 2019.
- [Tang *et al.*, 2021] Yunlei Tang, Sebastian Dorn, and Chiragkumar Savani. Center3d: Center-based monocular 3d object detection with joint depth understanding. In *DAGM German Conference on Pattern Recognition*, pages 289–302. Springer, 2021.
- [Tang *et al.*, 2022] Jiaxiang Tang, Xiaokang Chen, Jingbo Wang, and Gang Zeng. Not all voxels are equal: Semantic scene completion from the point-voxel perspective. In *Proceedings of the AAAI Conference on Artificial Intelligence*, volume 36, pages 2352–2360, 2022.
- [Wang *et al.*, 2020] Wenshan Wang, DeLong Zhu, Xiangwei Wang, Yaoyu Hu, Yuheng Qiu, Chen Wang, Yafei Hu, Ashish Kapoor, and Sebastian Scherer. Tartanair: A dataset to push the limits of visual slam. 2020.
- [Wu *et al.*, 2020] Shun-Cheng Wu, Keisuke Tateno, Nassir Navab, and Federico Tombari. Scfusion: Real-time incremental scene reconstruction with semantic completion. In *2020 International Conference on 3D Vision (3DV)*, pages 801–810. IEEE, 2020.
- [Yan *et al.*, 2021] Xu Yan, Jiantao Gao, Jie Li, Ruimao Zhang, Zhen Li, Rui Huang, and Shuguang Cui. Sparse single sweep lidar point cloud segmentation via learning contextual shape priors from scene completion. In *Proceedings of the AAAI Conference on Artificial Intelligence*, volume 35, pages 3101–3109, 2021.
- [Yang *et al.*, 2021] Xuemeng Yang, Hao Zou, Xin Kong, Tianxin Huang, Yong Liu, Wanlong Li, Feng Wen, and Hongbo Zhang. Semantic segmentation-assisted scene completion for lidar point clouds. In *2021 IEEE/RSJ International Conference on Intelligent Robots and Systems (IROS)*, pages 3555–3562. IEEE, 2021.
- [Ye *et al.*, 2019] Jingwen Ye, Yixin Ji, Xinchao Wang, Kairi Ou, Dapeng Tao, and Mingli Song. Student becoming the master: Knowledge amalgamation for joint scene parsing, depth estimation, and more. In *Proceedings of the IEEE/CVF Conference on Computer Vision and Pattern Recognition*, pages 2829–2838, 2019.

[Zheng *et al.*, 2022] Wu Zheng, Mingxuan Hong, Li Jiang, and Chi-Wing Fu. Boosting 3d object detection by simulating multimodality on point clouds. In *Proceedings of the IEEE/CVF Conference on Computer Vision and Pattern Recognition*, pages 13638–13647, 2022.